A method based on the ray structure of acoustic modes for predicting the liner performance in annular ducts with flow

Antoine Moreau[1], Sébastien Guérin[1], Stefan Busse[2]
[1] *German Aerospace Center, Institute of Propulsion Technology, Engine Acoustics Dept., Berlin*
Email: antoine.moreau@dlr.de, sebastien.guerin@dlr.de
[2] *Berlin University of Technology, Inst. of Fluid Mechanics and Engineering Acoustics, Germany*

Introduction

Acoustical liners are very effective noise reducing components of modern aeroengines. The predictive method presented here aims at being integrated into a tool dedicated to the design-to-noise of conventional and contra-rotating fans [4]. A schematic representation of the liner mounting in the inlet and bypass duct of a turbofan is shown in Fig. 1. The prediction is organised as follows: 1) The sound field generated by the fan is decomposed into acoustic modes (m, n) for a hard-walled duct with plug flow. 2) The ray structure of the acoustic modes is determined using the ray theory as detailed by Chapman [1]. 3) The attenuation of each mode is calculated in function of the polar and azimuthal angles of propagation (angles at which the rays impinge on the wall) and the number of bounces along the ray path: the procedure is similar to that proposed by Rice [7].

The reasons for using the ray theory are multiple. Besides its applicability to liners [7, 3], this approach can be used to estimate the transmission through a blade row [5], and also the far-field radiation patterns [1]. Compared to the exact analytical solution, the ray approach is intuitive, generally more flexible and should run faster which is important since the method is to be integrated in a design-to-noise loop. The validity of the present approach is encouraged by Rice's results [7] which showed a good correlation between propagation angles and liner performance even though there could be an underestimation of the liner damping in the immediate vicinity of the modal optimum impedance.

Ray-Theory

Ray structure of acoustic duct modes

The studied configuration is simplified to an annular duct with plug flow. The effect of swirl and boundary layer on the cut-on factor and ray path are neglected. Moreover it is assumed that the presence of the liner does not significantly modify the propagation angles and induces no mode scattering at the extremities. Chapman [1] showed that at high frequencies the ray path associated to a duct mode is piecewise linear outside a caustic cylindrical surface. Inside that domain, the rays are helical. Thus, modes can be expressed in terms of two angles of propagation. In presence of flow, the phase propagation and energy propagation angles are not equal. The first ones are required for the calculation of the attenuation per ray bounce whereas the second ones are used to calculate the number of bounces.

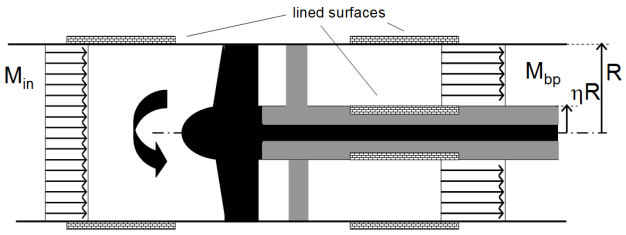

Figure 1: Schematic view of liner installation.

We assume a pressure disturbance in the form

$$p^{\pm}(x, r, \theta) = A^{\pm}_{mn} e^{i(k^{\pm}_{x,mn} x + m\theta - \omega t)} f_{mn}(r). \qquad (1)$$

The variables are described in Appendix. The cut-on factor α_{mn} is introduced, with

$$\alpha_{mn} = \sqrt{1 - (1 - M^2)\frac{\sigma^2_{mn}}{(kR)^2}}. \qquad (2)$$

For hard walls, the condition $0 < \alpha_{mn} \leq 1$ is verified by cut-on modes whereas α_{mn} is complex for cut-off modes.

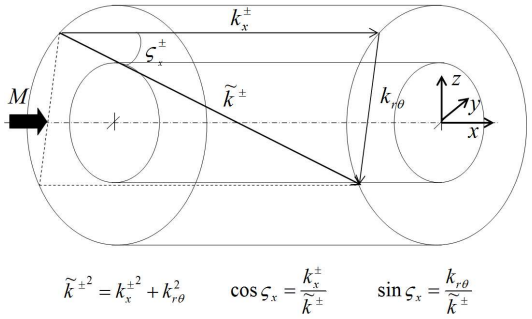

Figure 2: Phase propagation angle ζ_x.

Phase mode propagation angles

The angles of propagation are derived for a hard walled duct with uniform flow. The polar phase angle ζ_x is defined between the vector normal to the local wave front and the x-axis (see Fig. 2). It verifies the following relationships:

$$\cos\zeta^{\pm}_x = \frac{k^{\pm}_x}{\tilde{k}^{\pm}}; \qquad \sin\zeta^{\pm}_x = \frac{k_{r\theta}}{\tilde{k}^{\pm}}, \qquad (3)$$

and

$$0 \leq \zeta^{+}_x \leq \zeta^{-}_x, \quad \pi/2 \leq \zeta^{-}_x \leq \pi. \qquad (4)$$

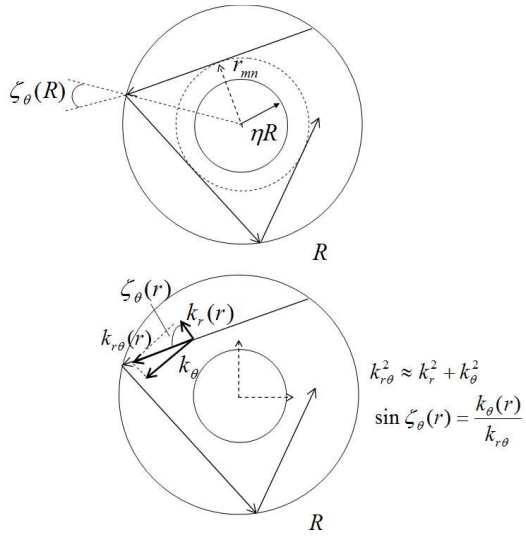

Figure 3: Phase mode propagation angle ζ_θ (The arrows represent the ray paths in the (r,θ)-plane).

The acoustical modes whose axial energy flux I_x is directed downstream (with flow) or upstream (against the flow) are distinguished by the symbols (+) and (−), respectively. The case $\zeta_x^+ > \pi/2$ means that the pressure wavefronts propagate upstreams (although the energy flux is in the positive direction). Moreover, it can be shown that

$$\cos\zeta_x^\pm = \frac{-M \pm \alpha_{mn}}{1 \mp \alpha_{mn} M}. \tag{5}$$

In the (r,θ)-plane, the phase angle ζ_θ represented in Fig. 3 verifies

$$\sin\zeta_\theta(r) = \frac{k_\theta(r)}{k_{r\theta}}. \tag{6}$$

Since $k_{r\theta} = \sigma_{mn}/R$ and $k_\theta(r) = m/r$, the value at the wall $(r = R)$ is

$$\sin\zeta_\theta(R) = \frac{m}{\sigma_{mn}}. \tag{7}$$

The angle $\zeta_\theta(R)$ has the same sign as m. It satisfies

$$-\pi/2 \le \zeta_\theta(R) \le \pi/2. \tag{8}$$

The angle ζ_r is defined between the component of the wave front normal to the wall, k_r, and the component of $\tilde{k}$ projected onto the (x,r)-plane. This angle is used in Eq.(18) to calculate the attenuation per bounce. The sinus of this angle is given by

$$\sin\zeta_r^\pm(r) = \frac{k_x^\pm}{\sqrt{k_x^{2\pm} + k_r^2(r)}}, \tag{9}$$

where

$$k_r^2(r) = \frac{1}{R^2}\left[\sigma_{mn}^2 - \left(\frac{R}{r}\right)^2 m^2\right]. \tag{10}$$

The angle ζ_r verifies

$$\zeta_r^- \le \zeta_r^+ \le \pi/2, \quad -\pi/2 \le \zeta_r^- \le 0. \tag{11}$$

Energy mode propagation angles

The energy mode propagation angles χ are associated to the group velocity vector. The polar angle χ_x verifies

$$\cos\chi_x^\pm = \frac{M + \cos\zeta_x^\pm}{\sqrt{1 + M^2 + 2M\cos\zeta_x^\pm}}, \tag{12}$$

hence using Eq.(5),

$$\cos\chi_x^\pm = \sqrt{(1-M^2)}\frac{\pm\alpha_{mn}}{\sqrt{1-\alpha_{mn}^2 M^2}}. \tag{13}$$

This is also the angle at which the peak of radiation is located in the far field with a uniform flow inside the duct and in its surrounding (see Eq.(27) of Rice, Heidmann, and Sofrin [6]). The following relationship is satisfied,

$$0 \le \chi_x^+ < \pi/2, \quad \chi_x^- = \pi - \chi_x^+. \tag{14}$$

The azimuthal angle of energy propagation is not modified since there is no swirl,

$$\tan\chi_\theta(R) = \tan\zeta_\theta(R). \tag{15}$$

Caustic radius

The caustic radius [1] outside which the ray paths are piecewise linear (see Fig.3) is given in Eq.(16).

$$r_{mn} = \frac{|m|}{\sigma_{mn}} R. \tag{16}$$

Since the intensity of the mode is predominantly located in the outer annulus $(r > r_{mn})$ (see Fig 4), the representation of acoutic modes through rays is legitimate.

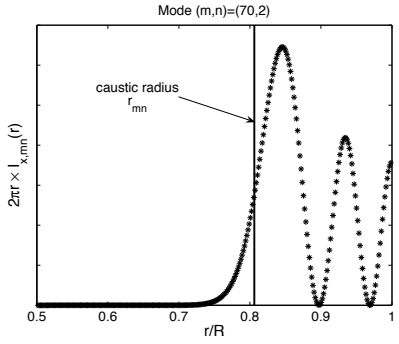

Figure 4: Radial distribution of the sound power ($\eta = 0.5$).

Liner damping

For a liner of length L, the number of bounces N is:

$$N = \frac{|\tan\chi_x^\pm|}{\cos\chi_\theta(R)}\frac{L}{2R}, \qquad \text{if } r_{mn} \ge \eta R,$$

$$N = \frac{2|\tan\chi_x^\pm|}{\cos\chi_\theta(R) - \sqrt{\eta^2 - \sin^2\chi_\theta(R)}}\frac{L}{2R}, \quad \text{if } r_{mn} < \eta R. \tag{17}$$

The second formula applies to acoustic modes whose caustic radius is smaller than the hub radius. These modes are reflected by the hub as well. As a consequence the number of bounces more than doubles for those

modes. Since $\chi_x^- = \pi - \chi_x^+$, the number of bounces is exactly the same for the modes propagating in the positive and negative directions. Moreover, the number of bounces dramatically increases for $\chi_x^\pm$ approaching $\pi/2$, i.e. for the modes that are near cut-off.

The ratio of the transmitted to the incident acoustic axial intensity for one bounce is obtained by [7]:

$$\frac{I^\pm_{ray,x,t}}{I^\pm_{ray,x,i}} = \frac{(\Theta^2+\Xi^2)\cos^2\zeta_r^\pm(r_w)(1+M\sin\zeta_r^\pm(r_w))^2}{(\Theta^2+\Xi^2)\cos^2\zeta_r^\pm(r_w)(1+M\sin\zeta_r^\pm(r_w))^2}\cdots \cdots\frac{-2\Theta\cos\zeta_r^\pm(r_w)(1+M\sin\zeta_r^\pm(r_w))+1}{+2\Theta\cos\zeta_r^\pm(r_w)(1+M\sin\zeta_r^\pm(r_w))+1}. \quad (18)$$

where $r_w = R$ at the casing or $r_w = \eta R$ at the hub. The peak angles of attenuation depend on the impedance and the flow velocity. After N bounces, the attenuation is

$$\begin{cases} \Delta = \left(\dfrac{I_{ray,x,t}}{I_{ray,x,i}}\right)^N_{r_w=R}, & \text{if } r_{mn} \geq \eta R, \\ \Delta = \left(\dfrac{I_{ray,x,t}}{I_{ray,x,i}}\right)^{N/2}_{r_w=R} \times \left(\dfrac{I_{ray,x,t}}{I_{ray,x,i}}\right)^{N/2}_{r_w=\eta R}, & \text{if } r_{mn} < \eta R. \end{cases} \quad (19)$$

Again the second formula has to be applied for modes whose caustic radius is smaller than the hub radius.

Results

Liner modal transfer function

An example of application is now presented for which more than 700 modes are cut-on. The following parameters are used: $M = 0.6$, $\eta = 0.5$, $kR = 50$, $Z = 1.5 - 0.47i$, $L = 1R$. As shown in Fig. 5, the number of bounces strongly increases for modes near cut-off and also is higher for modes whose caustic radius is smaller than the hub radius (see Eq.(17)).

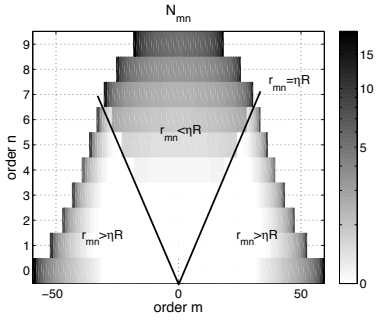

Figure 5: Number of bounces for a liner length of one radius ($kR = 50$, $M = 0.6$, $\eta = 0.5$).

Due to the axial mean flow, the attenuation per bounce is different for the upstream and downstream propagating modes. On the one hand, the peak angle of attenuation per bounce increases for both directions. On the other hand, the angles ζ_r^+ and ζ_r^- become smaller. In this particular example, the attenuation is stronger in the (+) direction as can be seen in Fig. 6 and 7.

We now investigate the role of the liner on the noise generated by a uniform radial distribution of uncorrelated dipoles directed at 45 deg with respect to the duct axis. As it can be observed in Fig. 8, some (m,n)-modes are not excited by this sort of source distribution. As shown in Ref. [2], these modes are such that the phase propagation angle is perpendicular to the dipole axis. After applying the liner transfer function, the modes near cut-off are strongly damped (Fig. 9).

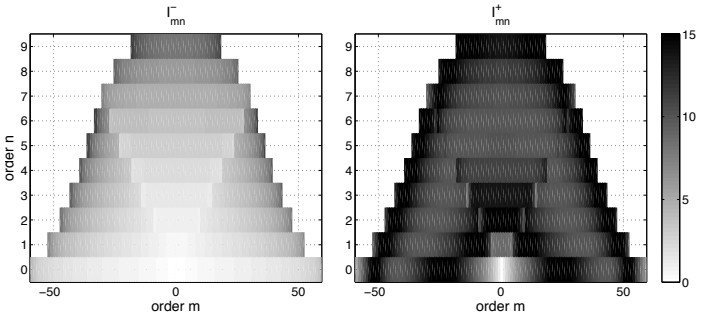

Figure 6: Sound attenuation (dB-scale) for $N = 1$.

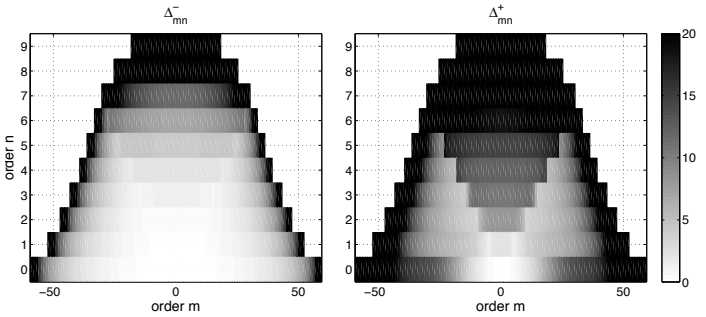

Figure 7: Total modal sound attenuation ($L = 1R$, dB-scale).

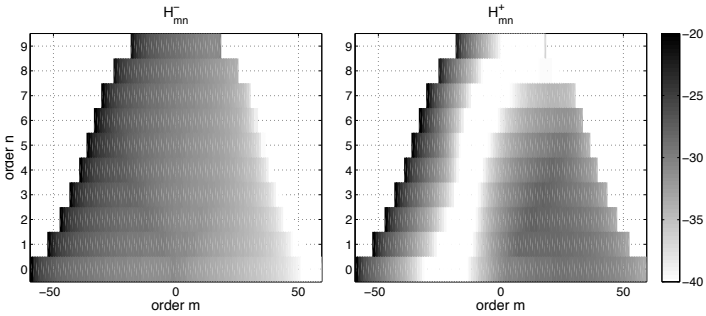

Figure 8: Modal tranfer function (dB-scale) of a radial distribution of uncorrelated dipoles oriented at 45 deg.

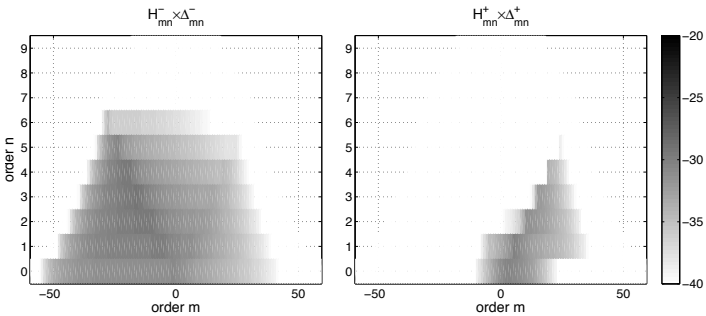

Figure 9: Modal tranfer function with liner.

Insertion loss

The last presented example (see Fig. 10) estimates the spectral attenuation of a liner whose impedance is frequency dependent ($Z(k) = 1.5 + i(0.01k - \cot(0.016k))$). The source model composed of radial distributed uncorrelated dipoles is applied along with the so-called equipartition of modal energy (EME) model for which all cut-on modes have the same energy. One configuration simulates the inlet ($\eta = 0$, $M = 0.45$) and the other the bypass duct ($\eta = 0.5$, $M = 0.6$) propagation. The attenuation curves follow an expected trend, i.e. have a null value for very low frequencies (only $(m, n) = (0, 0)$ is cut-on), increase up to a maximum for $kR \simeq 65$ when $\Xi = 0$, then decrease. Depending on the frequency range (actually on the impedance), the noise is more strongly absorbed either in the downstream or the upstream direction. The trend is the same for the two source models investigated. However the dipole distribution leads to a higher absorption because more energy is carried by the modes near cut-off which are well damped by the liner. Note also that the attenuation is improved with hub, which is partly due to the fact that the overall lined surface has increased by 50%.

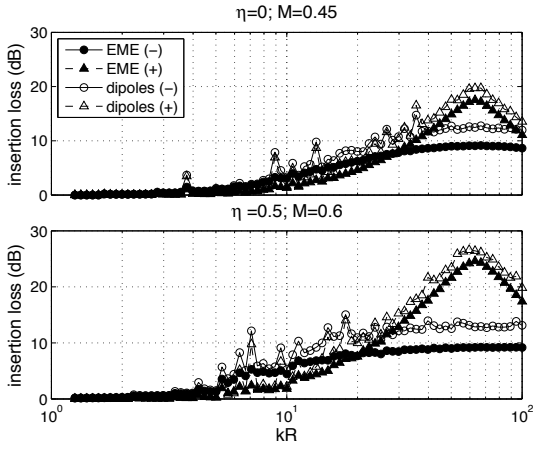

Figure 10: Insertion loss ($L = 1R$, $R = 1$ m, dB-scale).

Conclusion

With the objective of being used for the design-to-noise of turbofan engines, a simplified predictive model for the noise attenuation of liners was developed by combining the studies of Rice [7] and Chapman [1]. Both works deal with the ray theory. The solution was extended to annular ducts. Even though the first results look promising, they still have to be compared to the exact analytical solutions before the method can be applied with confidence. In particular, it would be interesting to study the influence of soft wall boundary conditions on the propagation angles of the rays. The error estimate will have to be conducted at realistic values of frequency for which generally many acoustic modes propagate.

Nomenclature

$f_{mn}(r)$	normalised mode shape function
H_{mn}	modal transfer function (see Ref. [2])
i	$i^2 = -1$
I_x	axial intensity
k	free-field wavenumber
$\tilde{k}^{\pm}_{mn}$	apparent wavenumber
$k^{\pm}_{x,mn}$	axial wavenumber
$k_{r\theta,mn}$	transversal wavenumber
k_r	radial wavenumber
k_θ	tangential wavenumber
L	liner length
M	axial Mach number (plug flow)
(m, n)	azimuthal and radial mode orders
N	number of bounces
p	pressure
R	duct radius
r_{mn}	caustic radius
(r, θ, x)	cylindrical system of coordinates
t	time
α_{mn}	cut-on factor
Δ_{mn}	modal attenuation
η	hub-to-tip ratio
σ_{mn}	eigenvalue
ζ	phase propagation angles
χ	energy propagation angles
Z, Θ, Ξ	liner specific impedance, resistance, reactance

References

[1] Chapman C.J., Sound radiation from a cylindrical duct. part 1. Ray structure of the duct modes and the external field, J. Fluid mech. **281** (1994), 293-311.

[2] Guérin S., Moreau A., Tapken U., Relation between source models and acoustic duct modes, 15th AIAA/CEAS Aeroacoustics Conference, 11-13 May 2009, Miami, Florida (USA), AIAA-Paper 2009-3364.

[3] Kempton A.J., Ray-theory and mode-theory predictions of intake-liner performance: a comparison with engine measurements, 8th AIAA Aeroacoustics Conference, Atlanta, Georgia (USA), April 11-13, 1983, AIAA-Paper 83-0711.

[4] Moreau A., Enghardt L., Improvements of a parametric model for fan broadband and tonal noise, Acoustics'08 Paris, 29 June-4 July 2008, Paris (France).

[5] Muir R.S., The application of semi-actuator disk model to sound transmission calculations in turbomachinery, part 1: the single blade row, J. Sound Vib. **54**(3) (1977), 393-408.

[6] Rice E.J., Heidmann M.F., T.G. Sofrin, Modal propagation angles in a cylindrical duct with flow and their relation to sound radaition, 17th Aerospace Sciences Meeting, new Orleans (US), January 15-17, 1979, AIAA Paper 79-0183.

[7] Rice E.J., Modal propagation angles in ducts with soft walls and their connection with suppressor performance, 5th AIAA Aeroacoustics Conference, Seattle, Washington (USA), March 12-14, 1979, AIAA-Paper 79-0624.